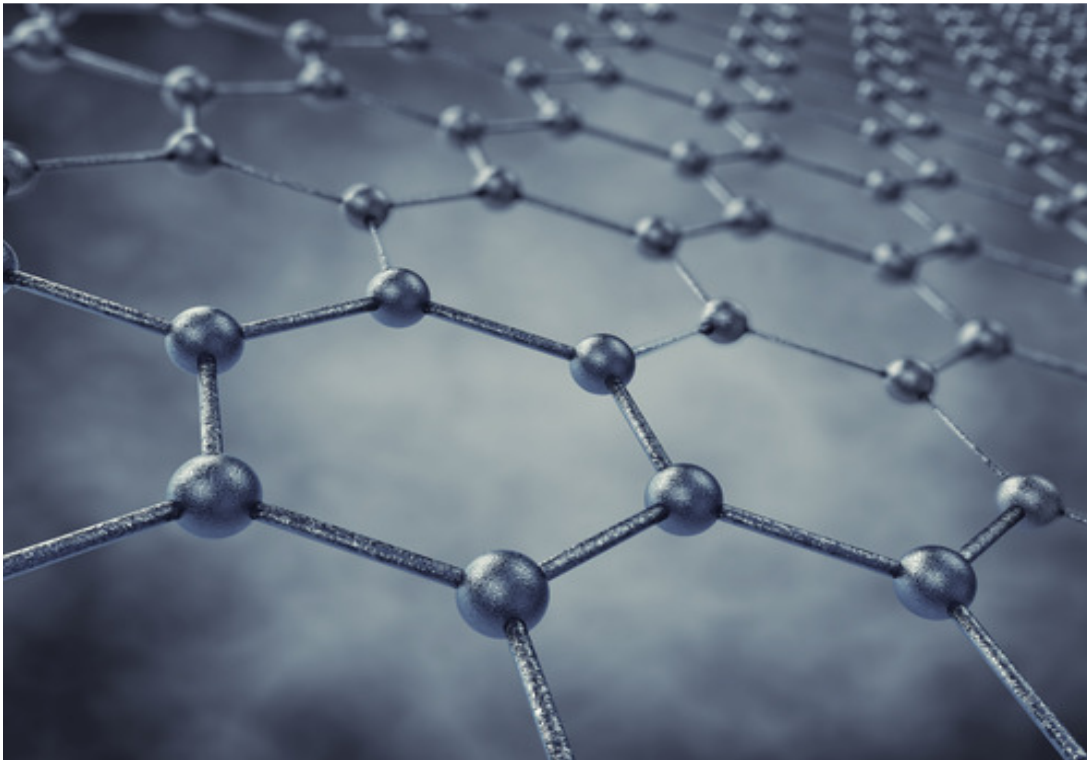# CHALMERS

Feasibility study of functionalized graphene for compatibility with cement hydrates and reinforcement steel

Master of Science Thesis in the Master's Program Structural Engineering and Building Technology

SOFIA SIDERI

Department of Civil and Environmental Engineering
Division of Building Technology
Building Materials
CHALMERS UNIVERSITY OF TECHNOLOGY
Gothenburg, Sweden 2014
Master's Thesis 2014:93

Feasibility study of functionalized graphene for compatibility with cement hydrates and reinforcement steel

Master of Science Thesis in the Master's Program Structural Engineering and Building Technology

SOFIA SIDERI

Department of Civil and Environmental Engineering
Division of Building Technology
Building Materials
CHALMERS UNIVERSITY OF TECHNOLOGY
Gothenburg, Sweden 2014

Feasibility study of functionalized graphene for compatibility with cement hydrates
and reinforcement steel

Master of Science Thesis in the Master's Program

SOFIA SIDERI

Department of Civil and Environmental Engineering
Division of Building Technology
Building Materials
Chalmers University of Technology
SE-412 96 Gothenburg
Sweden
Telephone: + 46 (0)31-772 1000

Cover: Graphene's structure

Department of Civil and Environmental Engineering Gothenburg, Sweden, 2014

Feasibility study of functionalized graphene for compatibility with cement hydrates and reinforcement steel

SOFIA SIDERI
Department of Civil and Environmental Engineering
Division of Building Technology
Building Materials
Chalmers University of Technology

Abstract

Cement-based concrete is a widely used material for a great variety of constructions. Although, cement has great properties and high performance, its intrinsic brittleness is a weakness that requires further investigation for improvement. Graphene demonstrates a number of excellent properties, such as high flexibility, 1 TPa Young's modulus, 130 GPa tensile strength, high electrical and thermal conductivity. This study investigated the feasibility of implementing graphene into the cement matrix for improving its compressive and tensile or flexural strength. In addition, graphene coating was also investigated for protecting reinforcement steel bars in concrete from corrosion.

Within the framework of this study, three main tests were conducted: compressive tests and tensile test on specimens of cement paste and mortar containing graphene, and half-cell potential test on corrosion initiation of steel bars coated with graphene and embbeded in cement mortar.

From the literature, several research studies indicate the significance to investigate the graphene and its derivatives with cement composites within a multi-scale approach. According to one of the studies addition of graphene oxides (GO) with 1.5% by weight of cement revealed an increase in tensile strength by 48% compared with the cement mixture without graphene oxides. The Field Emission Scanning Electron Microscopy (FE-SEM) images showed good bonding between GO and the cement particles. The results obtained from the experimental study of this master thesis work did not, however, reflect graphene's potential due to the fact that the functionalized graphene used in this study contained functional groups with silicon oxides, which were polymerized and inactive for chemical interaction with the cement hydrates.

The study results from the literature also proved that single but also multi-layer graphene can work as anti-corrosion coating. The corrosion test from this master thesis work indicated that the specimens with graphene coating revealed a delayed corrosion initiation and some repassivation-depassivation cycles, as a result of the higher amount of chlorides needed for the depassivation of the passive film.

Key words: Cement, hydrates, graphene, reinforcement steel, corrosion, functionalized graphene, graphene nanoparticles.

Table of contents

CHALMERS, *Civil and Environmental Engineering*, Master's Thesis 2014:93

Preface

Graphene and its applications to building materials such as cement and concrete attracted my research interest. Therefore, I carried out this feasibility study as my master examination work.

The experiments have been carried out from January to May 2014. The project was carried out at the laboratory of Chalmers University of Technology, Sweden.

I would like to thank my supervisors, Professors Tang Luping and Liu Johan for their support. I would also like to thank the Bio-Nano Laboratory of MC2 and Smart High Tech AB for providing us with graphene.

Many thanks are extended to my family that supported me all the way to complete my studies.

Gothenburg, June 2014

Sofia Sideri

1. Introduction

1.1 Background

Cement-based concrete is the most commonly used material in civil infrastructure. Although cementitious materials have shown great properties, they are also quasi-brittle materials with very low tensile strength and reduced strain capacity.

The research aims to address the weaknesses of cement in different ways. Scientific research is conducted in different directions. The most prevalent research method gives emphasis on a bottom-up approach of the problem with a multiscale evaluation from atomic level to nanoscale, then microscale and finally mesoscale level. (Alkhateb et al., 2013)

According to Sobolev and Gutierrez (2005) nanotechnology can change the world and specifically for cement-based materials, focusing on their structure at the nanoscale will possibly give us more information on how we could improve its characteristics. As a result, concrete could become stronger with increased durability, increased strain capacity and other innovative properties. Later on, Sobolev and Shah (2008) suggested that with the development of nano-technology new generation of cementitious materials could be produced in the future:

- 'cement-based materials with engineered nano and micro structures could exhibit supreme durability'
- 'Self-healing materials and repair technologies utilizing fullerenes , nanoparticles, nanotubes, nanotubes and chemical admixtures'
- 'Self-cleaning, non- shrinking and low thermal expansion materials or even smart materials such as temperature-, moisture-, stress- sensing materials.'

Recent research has indicated that using nanomaterials (carbon nanotubes, graphene, titanium oxide, nanosilica and nanoalumina) can significantly improve cementitious materials. However, the high cost and the time-consuming procedure of production are very important factors that need great consideration.

Such research for graphene has shown that there is strong connection between the structure and the performance of graphene-cement nanocomposites (GCNCs). The functionalized graphene-nanoplatelets had improved interfacial strength, which in turn ameliorates their mechanical properties (Alkhateb et al., 2013). Introduced graphene nanoparticles in the cement paste showed that this change in microstructure improved its thermal and electrical diffusivity, which means that micro-cracks due to the exothermic hydration process can be avoided and also graphene could be used for electrostatic dissipation of charge (ESD) (Sedaghat et al., 2014).

Babak et al., (2014) highlighted in their research article that cement mortar with 1.5% Graphene Oxide (GO) had 48% increase in its tensile strength and also that there was

2

good bonding between the GO surfaces and the cement matrix. X-ray diffraction (XRD) data also showed that the mortar with GO had increased calcium silicate hydrates (C-S-H) gels in comparison with normal cement mortar.

As far as it concerns this master thesis, a feasibility study was conducted in order to investigate the compatibility of the functionalized graphene with the cement hydrates and the reinforcing steel.

Graphene could possibly integrate into the cement paste or mortar and strengthen the bonds of the cement hydrates. As a result, the fundamental properties of cement and especially its tensile and compressive strength could be improved. In addition, graphene was also used as steel coating on reinforcement bars in order to check their compatibility and graphene's electrical conductivity could also help in eliminating the local chloride accumulation and protect the re-bars from corrosion.

1.2 Purpose and objectives

The main purpose of this thesis is to investigate the feasibility of functionalized graphene for compatibility with cement hydrates and reinforcement steel. The main objectives of this thesis are:
1) Literature study of cement bonds with nano-materials such as graphene and their properties
2) Investigation of the compatibility by testing compressive and tensile strength of hardened cement specimens mixed with graphene.
3) Investigation of the compatibility by testing the corrosion sensitivity of reinforcement steel bars coated with graphene.

1.3 Method

The master thesis consists of two parts: the first part covers the literature study and the second part covers the experiments conducted. In the first part, the following chapters are analysed: the cement hydration products, the graphene's structure and their possible bonds,

At the second part the experiments are analysed. These are compressive strength, tensile strength and corrosion tests.

2. Cement-graphene compatibility

2.1 The atomic structure of C-S-H gel

To further understand the mechanism of cement hydrates making bonds with the graphene, it is crucial to investigate cement's hydration. After mixing the cement powder with water, a myriad of chemical reactions happen and a rigid, complicated and porous material is formed, called cement paste.

Actually, the cement paste can be also described as a composite material consisted of calcium hydroxide crystals (portlandite), aluminates and non-hydrated cement, and an amorphous gel called C-S-H (Calcium-Silicate-Hydrate) gel. This gel dominates the most important hardened properties of cement paste, such as its strength and stiffness.

Several models have been proposed for modelling the C-S-H gel's nanostructure. C-S-H has a crystalline structure but it has elements and pores of several sizes. Some studies stated either that C-S-H has an amorphous structure (Damme et al., 2006) or that C-S-H has crystalline structures (Manzano et al., 2007).
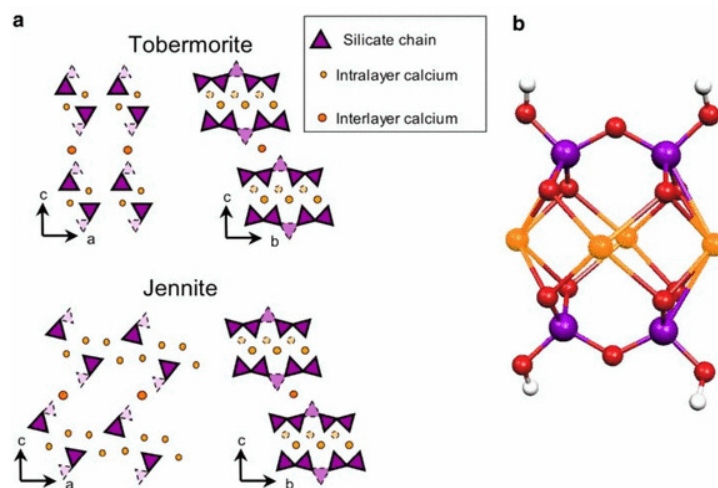
Fig. 2.1 Atomic models of the tobermorite and jennite crystals (Manzano et al., 2007)

There are more than 30 different crystalline structures mainly represented by the 14-Å tobermorite and jennite. The amorphous gel structure is very difficult to model. C-S-H gel is often referred with its Ca/Si ratio, which varies between 0.7 to 2.3. This high variability explains the reason why the extensive research conducted so far has not given a precise picture of the C-S-H nanostructure or how we could reinforce and enhance its properties. Besides that, the chemical composition varies within the cement paste. Thus, in order to investigate the nanostructure of C-S-H, more parameters need to be investigated such as: the variations of the Ca/Si ratio, silicate structure, and contents of Si-OH and Ca-OH (Chen et al., 2004).

Tobermorite has Ca/Si ratio of 0.83 and density of 2.18 g/cm^3, whereas Jennite has Ca/Si ratio of 1.5 and density of 2.27 g/cm^3. Richardson (1999) introduced two models for the C-S-H gel's structure: the tobermorite/jennite (T/J) models and the tobermorite/calcium hydroxyl (T/CH) models. In addition, Richardson (1999) suggested that the C-S-H gel structure may have glass-like and crystalline properties due to the mineral tobermorite. The atomic structures proposed were: 14-Å $Ca_5Si_6O_{16}(OH)_2 \cdot 7H_2O$ for tobermorite and $Ca_9(Si_6O_{18})(OH)_6 \cdot 8H_2O$ for jennite.

The tunnelling electron microscope (TEM) showed that the shape of C-S-H resembles disks of 5 nm thickness. During the hydration phase, C-S-H gels are classified in two categories depending on their density: (HD) High Density C-S-H gels and (LD) Low Density C-S-H gels, which also have different mechanical properties. The ratio of high density to low density C-S-H gels depends on the design of the mixture.

Jennings (2000) suggested that C-S-H gels have a colloidal structure with different packing densities. Increase in the packing densities means higher number of contacts between the particles of the cement paste. The HD C-S-H gels have greater stiffness and hardness due to the fact that they have more contacts between the particles.

2.2 The atomic structure of graphene and GO

Graphene originally comes from single-layer carbon atoms well-packed in a 2D honeycomb lattice and is the main element for the synthesis of all the other graphitic materials of all dimensions. It can be found closed in 0D fullerenes, wrapped in 1D nanotubes or stacked in 3D graphite (Geim et al., 2007).
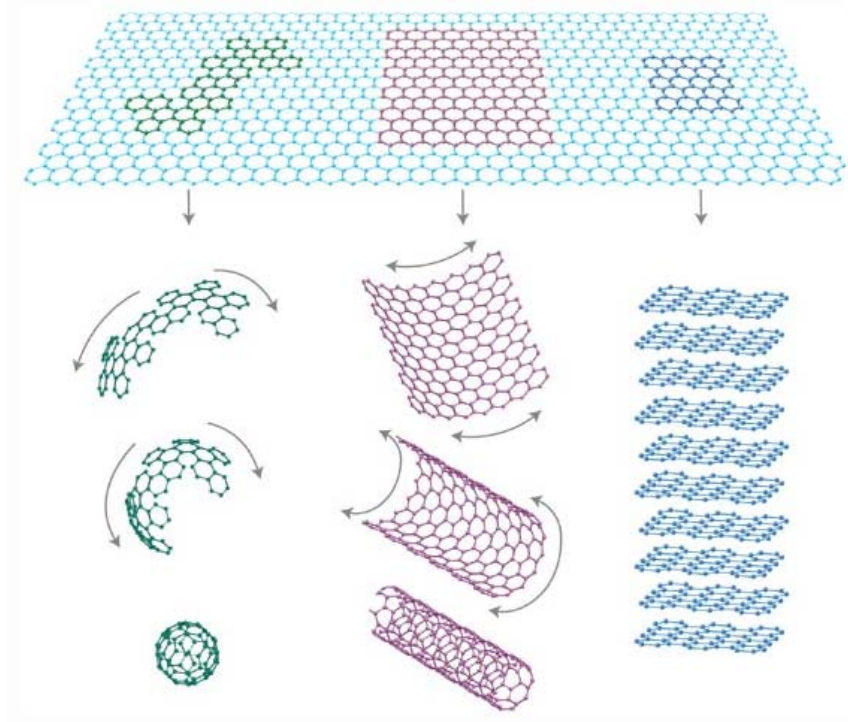
Fig. 2.2 Graphene as a 2D building material for carbon materials of all types of dimensions: 0D buckyballs, 1D nanotubes or stacked in 3D graphite. (Geim et al., 2007)

The atomic structure of graphene can be easily understood if the elemental carbon and its 3D allotropes are studied. The atom of carbon has atomic number 6, which means that its atomic orbitals are: $1s^2$, $2s^2$, $2p_x^1$ and $2p_y^1$. The atom of carbon is tetravalent, which means that only the four exterior electrons participate in covalent bonds.

The following figure shows the atomic orbital diagram of a carbon atom at ground state (case a) and later on hybridized to sp^3 form (case b) of the diamond and the hybridized sp^2 form (case b) of the graphite and graphene (Warner et al., 2013).

Fig. 2.3 The atomic orbitals of carbon element (Warner et al., 2013)

Graphene is a 2D layer material and has one atom thickness, sp^2 covalent bonded carbon atoms, which form a honey-comb crystal lattice. The intrinsic strength of graphene is 130 GPa and its Young's modulus is 1 TPa according to nanoindentation atomic force microscopy(AFM) for a single layer graphene sheet (Lee et al., 2008). Graphene's planar structure is beneficial for bondings on the upper and bottom surface in close distance with the hosting material. The theoretical specif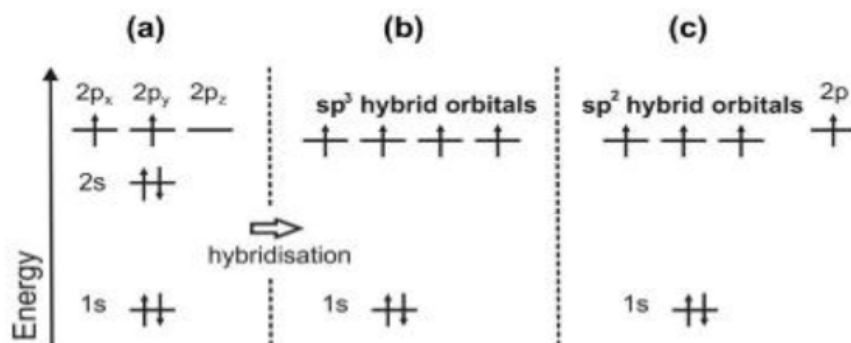ic surface area of a single sheet of graphene could be 2630 m^2/g, which is even higher than that of carbon nanotubes (Zhu et al., 2010, Peigney, 2001). The bigger the surface area is, the more possible it becomes to interact physically and chemically with the host material and enhance the bondings formed between these two materials. Although, graphene is extremely attractive due to its remarkable properties, there is significant difficulty to produce more than small quantities and lower the cost of production in order to facilitate its massive production and industrial application (Alkhateb et al., 2013).

For this reason, Graphene Oxide (GO), which is a graphene derivative has been examined as an alternative nanomaterial to graphene. Graphene Oxide is also a single layer material of sp^2 hybridized carbon atoms derivatized by a mixture of hydroxyl and epoxy functional groups (Warner et al., 2013). The following figure shows the graphene oxide structure with its oxygen, hydroxyl and carboxyl functionalities above and under the basal plane according to Lerf's schematic model (Lerf et al., 1998).
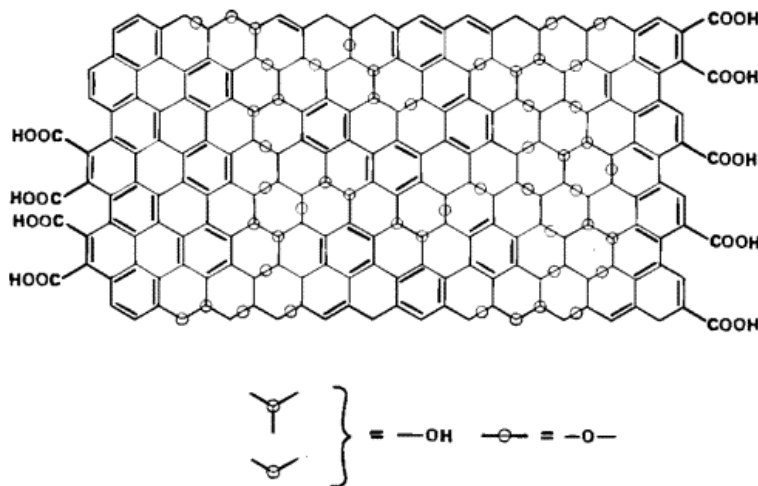

Fig. 2.4 Graphene oxide structure with its oxygen, hydroxyl and carboxyl functionalities (Lerf et al., 1998).

2.3 Morphological relationships between the fresh cement paste and graphene

Well-dispersed graphene and good interfacial interactions between the graphene nanoparticles and the cement matrix are essential for succeeding increase of mechanical and physical behavior of cement paste.

It is difficult for graphene and other graphite nano-materials to be well-dispersed into the cement matrix, since the cement's particles are in the micro-scale in an aqueous solution. The hardened cement paste includes micro- to nano-sized pores, which also limit the contact surface area of graphene with the cement hydrates. Graphene and other graphite nanomaterials could take the space between the micro-sized particles of the cement paste. To achieve thorough dispersion in the cement matrix, micro-scale cement particles could be partially replaced by silica fume nano-particles. This way, the particle size distribution would be improved and uniform dispersion would be achieved.
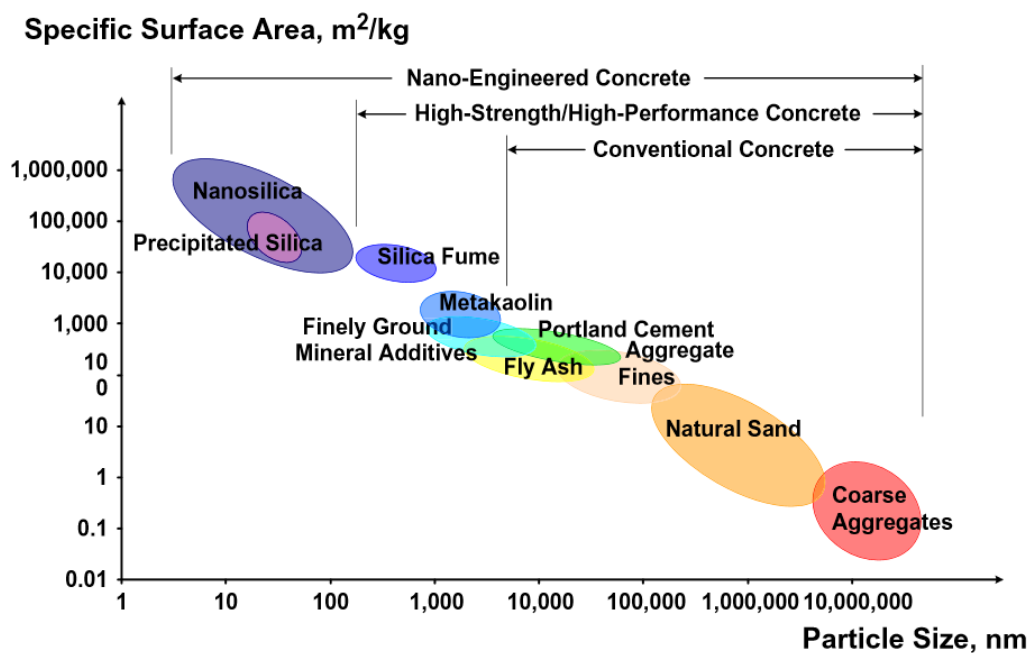
Fig. 2.5 Particle size and specific surface area related to concrete materials. (Sobolev et al., 2005)

During hydration, the cement particles react with water and conceive partially the space between them. The rest space is occupied by the remaining water and micro-scale capillary pores are formed. The hydrated cement consists of: C-S-H particles (where the main binding force between them is Van der Waals bonds), micro-scale C-H crystals, capillary pores and gel pores with calcium silicate hydrate and other hydration products.

The water/cement ratio affects the amount of capillary pores in the hydrated cement paste. In addition the calcium hydroxide micro-scale C-H crystals' specific surface area is smaller than the other hydration products, thus their ability to make bonds with graphene is limited. Hence, the presence of micro-scale pores and crystals limits the interaction of graphene and hydrated cement particles.

Better particle size distribution of the fresh cement paste and also use of superplasticizers (surfactants) to increase the cement's workability and use less water (thus dense cement) would refine the micro-morphology of cement and improve graphene's reinforcement efficiency.

Functionalization of graphene and its derivatives could improve their compatibility with the cement hydrates, forming stronger chemical bonds (Sadiq, 2013). Functionalized graphene could benefit both its dispersion in aqueous solution and reinforce the interfacial bondings with the cement hydrates. However, functionalization techniques should be further improved in order not to excessively damage the graphene's structure.

2.4 Graphene functionalization

Among the fabrication methods of graphene, chemically oxidized graphene (Graphene Oxide-GO) is widely used as starting material in favor of its good dispersion, bulk production and unique multifunction properties (Wei et al., 2012).

When graphene is produced from GO it is already functionalized but the residual oxygen-containing functional groups are not enough to maintain the surface area needed for stable dispersion in the solvents. For this reason, graphene oxide's surface should be further modified in order to be well-dissolved and also have better interfacial interaction with the cement hydrates.

Graphene can be functionalized with three different methods; each one having advantages and disadvantages:

1) Non-covalent attachment of large/small aromatic-containing molecules through π-π stacking

⊕ There is no high damage because of the functionalization.

⊖ Weak bonds are developed, thus the load bearing capacity of the composites is quite low.

2) Grafting molecules on the basal plane of graphene

⊕ Strong bonds are created between graphene and the attached molecules.

9

⊖ Defects are introduced on the graphene surface, thus the graphene's structure is weakened.

3) Chemical reactions between the functional groups on GO and other molecules, together with subsequent or simultaneous chemical reduction

⊕This method overcomes the problems of method 1) and 2) through chemical bonding.

⊖ Not suggested method for graphene produced by thermal exfoliation (>550°C) (Hsiao et al., 2010) .

The research groups of Boukhvalov & Katsnelson (2008) and Gao et al. (2010) after using the density functional theory, both groups concluded that it was impossible to produce graphene without oxygen-containing functional groups using either chemical or thermal reduction.
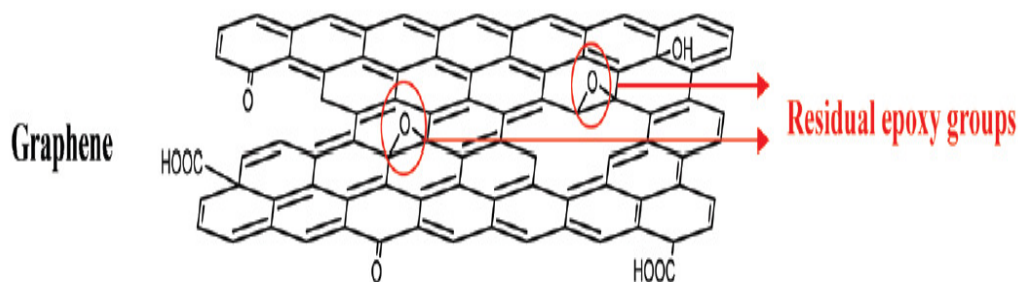
Fig. 2.6 The residual epoxy groups on graphene after thermal or chemical reduction, (Hsiao et al., 2010)

For this reason, it was suggested that the residual oxygen-containing functional groups could be used for covalent functionalization. The residual functional groups attached to the graphene oxide's surface, such as hydroxyl, epoxy, carbonyl, carboxylate groups, etc. could react with other functional groups grafted on the desirable molecules. This method does not harm the graphene structure and provides higher thermal stability than grafting molecules on the basal plane of graphene (Hsiao et al., 2010).

Another research study from Petrunin et al. (2013) investigated the performance of cement composites with functionalized multi-walled carbon nanotubes. The multi-walled carbon nanotubes were functionalized with carboxylic groups by grafting on their surface. The compressive strength test results showed 20% increase in the composite with 0.13% wt (of cement) over the reference after 28 days of curing. Also, the carboxilated MWCNTs with 0.05% wt (of cement) showed 30% increase after 1 day of curing. Thus, the functionalized carbon nanotubes accelerated the cement hydration of Portland cement, thus its early strength. However, the unmodified MWCNTs showed greater compressive strength after 28 days.

2.5 Graphene-cement nanocomposites

To investigate the effects of graphene and its derivatives on the cement's overall response a multiple approach from nano-level to micro-level is needed in order to identify the 3D model of its structure and observe the interactions between graphene and cement particles.

The graphene nanoparticles are expected to improve the cement matrix in a nanoscale and therefore its microscale structure. There has been a lot of research focused on single wall carbon nanotubes and multiwall carbon nanotubes, as well as on their functionalization and the carbon nanofibers, but little research has been conducted on graphene functionalized with functional groups, which would participate in bonds with the cement oxides. Hence, there is great need for further research to broaden our knowledge on the mechanical, thermal and physical behaviour of the graphene-cement nanocomposites.

With respect to previous research studies, graphene embedded to the cement matrix is expected to improve cement's toughness and more specifically its tensile, compressive, or bending and interfacial strength. The functionalization of graphene using the remained oxygen atoms of functional groups or grafting the desirable molecules to react with the molecules expected to make the bonds with cement particles is a new field of interest in the graphene-cement nanocomposites that may change the future of their civil engineering applications.

2.6 Previous studies - Research results

Several research studies indicate the significance to investigate further the graphene and its derivatives with cement composites within a holistic approach. It's an issue that requires multi-scale, chemical and atomistic study.

- ➢ Konsta-Gdoutos et al. (2010) used MWCNTs to investigate their reinforcing effect on the cementitious matrix. According to their study, the cementitious matrix showed improved fracture resistance properties. Additionally, the MWCNTs increased the high stiffness of C-S-H gel produced and decreased its porosity. The MWCNTs seem to reduce significantly the capillary stresses because of their small diameters (20-40 nm), thus improving the early strain capacity of the cement nanocomposites. Hence, the MWCNTs cement nanocomposites present early age and long term durability.
- ➢ Babak et al., (2014) investigated the potential of GO to improve the mechanical properties of cement nanocomposites. According to their study

CHALMERS, *Civil and Environmental Engineering*, Master's Thesis 2014:93

addition of GO by 1.5wt%(of cement) with 0.5 wt% superplasticizer showed 48% higher tensile strength compared to cement matrix without GO. The FE-SEM images showed good bonding between GO and the cement particles. Also, the XRD diffraction data revealed increased amount of C-S-H gel at the cement nanocomposite compared with pure cement mortar.

➢ Alkhateb et al. (2013) investigated the effects of functionalized graphene nanoplatelets on cement. They simulated the atomic models of G, G(OH), G(NH$_2$), G(COOH) as it can be seen in the following figures.
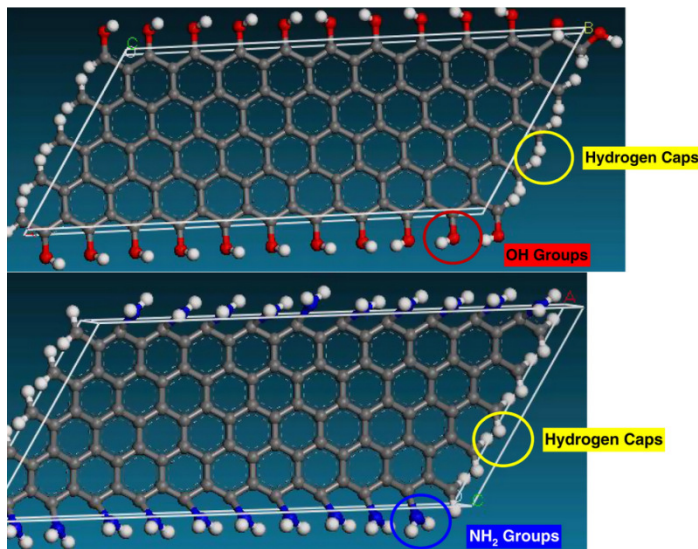
Fig. 2.7 Atomic model of G (OH) and G (NH$_2$) functionalized graphene (Alkhateb, 2013)

The interfacial bonding strength was calculated as the difference between the energy of the composite and the individual energies of the composite elements:

$\Delta E = E_{total} - (E_{fiber} + E_{matrix})$ and the energy difference was in all cases negative, which means that the compound was energetically favorable. The interaction energy mainly came from the Van der Waals and electrostatic interactions between C-S-H and graphene nanoplatelets. The magnitude of the energy difference is defined by the electrostatic energy interactions and the polarity of the functional groups of graphene.

Table 2.1 The interfacial strength between GCNCs and C-S-H gel

Composite	Interfacial strength (GPa)
(C-S-H)-G()-C-S-H	1.2
(C-S-H)-G(OH)-C-S-H	13.5
(C-S-H)-G(NH2)-C-S-H	6.1
(C-S-H)-G(COOH)-C-S-H	11.8

As it can be seen from the table above the interfacial strength of the G (OH) cement nanocomposite was calculated much higher than that only with graphene G().

3. Graphene coating for reinforcement steel

3.1 Mechanisms of chloride transport in concrete

Concrete is a porous material and its pore structure depends on several factors, such as: the water/cement ratio and the curing temperature. The pore system could be categorized in three main types: the gel pores with size of 1-10 nm, the capillary pores with size of 10 nm-10 μm and macropores and air voids of 10 μm till few mm. The gel pores have such a small size, which doesn't facilitate the chloride transport process and also the macropores and air voids have little significance with regards to sorption. The capillary pores and their connectivity determines the transport of ions, moisture and gases related to the corrosion of steel, i.e. its permeability.

The chloride transport mechanisms in concrete are:

- Capillary suction: takes place in dried or partially dried concrete, which has contact with water (dissolved ions) because of the surface tension in the capillary pores.
- Diffusion: takes place when concrete is saturated due to concentration gradients.
- Migration: is a transport of ions when electrical field is applied.

Factors affecting the chlorides transport are the RH, their interaction with the cement paste, the presence of cracks and the interfacial transition zone between cement paste and aggregates.

3.2 Corrosion is an electrochemical process

Water and oxygen are needed to initiate the corrosion process. The following two main redox reactions show the anodic oxidation of iron and the cathodic reduction of oxygen.

$$Fe \longrightarrow Fe^{+2} + 2e^{-} \tag{3.1}$$

$$H_2O + 1/2 O_2 + 2e^{-} \longrightarrow 2OH^{-} \tag{3.2}$$

One of the corrosion products from the above reactions is:

$$Fe + H_2O + 1/2 O_2 \longrightarrow Fe(OH)_2 \tag{3.3}$$

The environment of steel in concrete differs a lot from the one in wet corrosion of metals. In this process the steel comes in contact with the pore water which is highly alkaline, with pH around 12.5-13 because there is $Ca(OH)_2$ from the cement hydration and the oxides Na_2O and K_2O. The steel reacts with the pore water but instead of having the Fe^{+2}, Fe_3O_4 is formed on the metal as a thin film of a few nanometers thickness. This film stops the corrosion process and the steel is called passive. Thus, the concrete's reaction with the steel acts likes a protection from further corrosion.
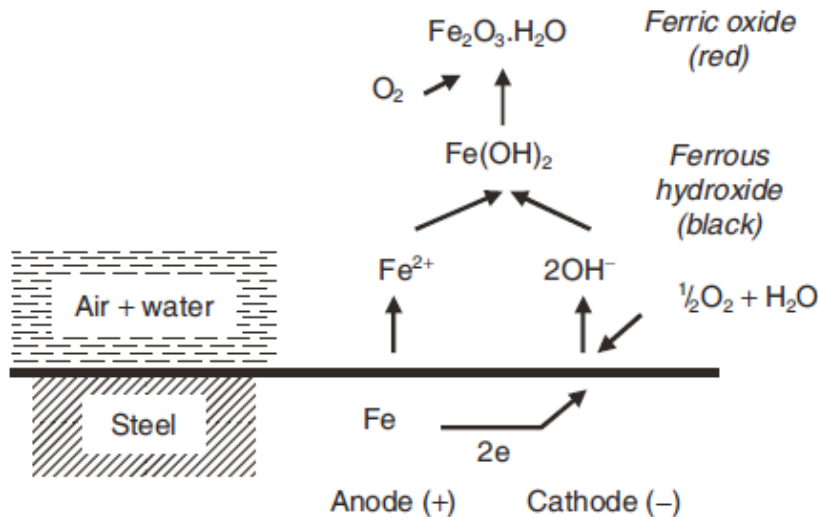
Fig. 3.1 The corrosion reactions on the iron surface in aerated water (Domone et al., 2010).

But, the alkalinity of the concrete is often destroyed by the phenomenon of carbonation or the chloride ingress. The carbonation process disturbs the highly alkaline environment of concrete from pH of 12.5-13 to about 8 and finally depassivates the steel. The carbon dioxide CO_2 reacts with $Ca\ (OH)_2$ and other hydroxides. As a result, calcium and other carbonates are produced. The presence of ions at the de-icing salts used during the winter periods or in the seawater can also destroy the passive film and cause pitting. Pitting is followed then by the corrosion reactions of the figure above.

Although, there have been a lot of studies conducted on the steel corrosion mechanisms, it is difficult to understand the mechanism of the breakdown of the passive film. There are three mechanisms usually corresponding to the breakdown of the passive film:

- the penetration mechanism: the high potential difference at the passive film lets the chloride ions to cross the passive film and reach the steel surface.
- the film breaking mechanism: the chloride ions penetrate the passive film due to cracks and defects on it.

- the adsorption mechanism: the chloride ions are adsorbed on the passive film and make it thinner until it finally breaks down. (Strehblow, 2002).

The following figure represents the pitting corrosion of reinforcement steel in concrete.
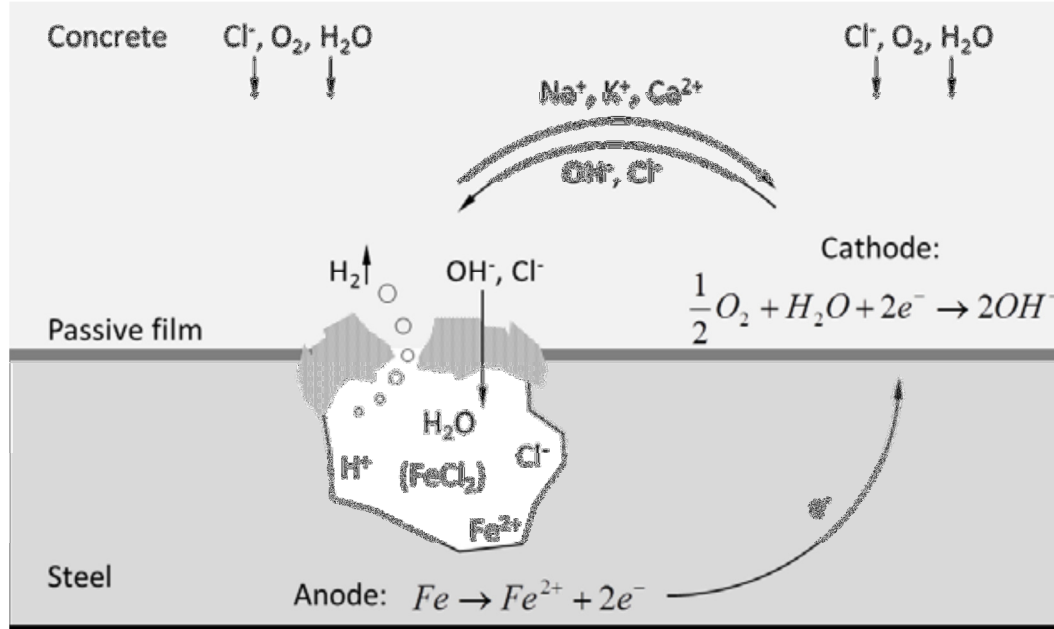
Fig. 3.2 The pitting corrosion of reinforcement steel embedded in concrete (Silva, 2013)

Finally, when the passive film breaks down a number of reactions take place: the anodic oxidation of steel and the oxygen reduction as explained before. This interruption of the electrical neutrality from the positive charges of Fe^{+2} causes an ionic current through the corroding point - anode, where the anions OH^-, Cl^- are moving to and the cations (Na^+, K^+, Ca^{+2}) are moving away from.

While, the iron ions Fe^{+2} react with water and produce several oxides and ferrite hydroxide, as in the reactions below:

$$Fe^{+2} + 2H_2O \rightarrow Fe(OH) + 2H^+ \tag{3.4}$$
$$2Fe^{+2} + 3H_2O \rightarrow Fe_2O_3 + 6H^+ + 2e^- \tag{3.5}$$
$$3Fe^{+2} + 4H_2O \rightarrow Fe_3O_4 + 8H^+ + 2e^- \tag{3.6}$$

According to Alvarez and Galvele (1984), Cheng and Luo (1999), after the reactions porous agglomerate is formed at the pit, which consists of iron rust and remains of the passive film. This agglomerate limits the mass transport through the pit.

In case the concrete is situated in an alkaline environment, the OH^- will penetrate into the pit and react with the H^+ (produced from the reactions above) in order to reach electrical balance and therefore repassivation.

CHALMERS, *Civil and Environmental Engineering*, Master's Thesis 2014:93

Inside the pit, there is high amount of chloride ions which react with water and produce hydrochloric acid:

$$3Fe^{+2} + 4H_2O \rightarrow Fe_3O_4 + 8H^+ + 2e^- \tag{3.7}$$

The hydrochloric acid lowers the pH value of the pit and it is possible to have hydrogen reduction: $2H^+ + 2e^- \rightarrow H_2$ (Pickering and Frankenthal, 1972). Then, the reactions in the pit continue, since the pit works as anode and cathode at the same time and the hydrogen production may cause embrittlement of the steel (Arup, 1983).

3.3 Electrochemical measurement techniques

There are two electrochemical measurement techniques: the open circuit potential (or half-cell potential) measurements and the potentiostatic measurements.

<u>Open circuit potential or half-cell potential measurements</u>

In open circuit potential experiment, the corrosion potential is measured i.e. the potential of a potentially corroding steel surface in an electrolyte, relative to a reference electrode e.g. saturated calomel electrode (SCE). The reference electrode is placed on the concrete surface attached to a wet sponge between them in order to have an electrolyte connection, or it can be place in the solution. The working cable is connected to a high impedance voltmeter (>10 MΩ) and the reference cable is connected to the ground terminal of the voltmeter. There are several reference electrodes for concrete measurements, thus the potential should be converted using the following conversion factors of the table below. The depassivation of the steel is identified by a sudden drop of the corrosion potential towards the more negative level.

Table 3.1 The standard Reference Electrode Potentials used in concrete (Vennesland, 2007).

Reference Electrode Potential	(mV *vs* SHE)
Copper/Copper Sulfate, $Cu/CuSO_4$	+316
Saturated Calomel	+244
Silver/Silver Chloride, Ag/AgCl	+199

In Table 3.1 the abbreviation SHE means Standard Hydrogen Electrode.

Figure 3.3 shows the variation of potential in different states of concrete. Specifically, the passive aerated concrete has potential of -200 to +100 mV vs. SCE (Bertolini et al., 2004).
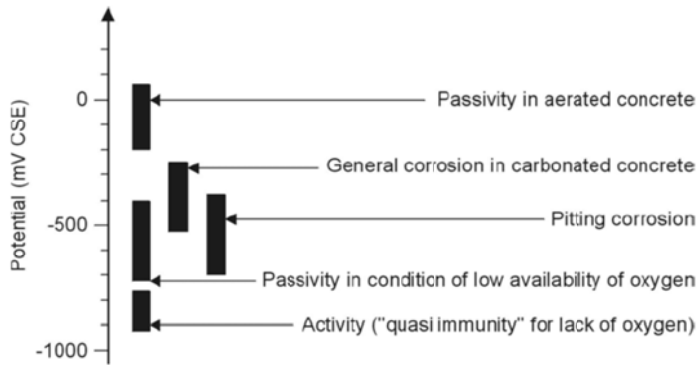
Fig. 3.3 Variation of potential in different states of concrete (Bertolini et al., 2004).

Potentiostatic measurements

As it can be seen in Figure 3.4 the potentiostat maintains the potential at constant level E_{corr} and is connected with a counter electrode immersed in the chloride solution, the steel bar works as a working electrode and a reference electrode immersed in the solution. The current passing through the working cable and the counter electrode in order to maintain the corrosion potential constant is measured. The depassivation of steel is identified when a sudden increase in the current occurs.

Fig. 3.4. Potentiostatic measurements on steel immersed in chloride solution (Silva, 2013).

3.4 Electrochemical rehabilitation methods

Electrochemical rehabilitation methods have been developed in order to reverse the steel corrosion and hence prolong the service life of steel used in concrete structures. There are three electrochemical rehabilitation methods:

- cathodic protection (CP),
- electrochemical chloride extraction (ECE)
- electrochemical realkalization (ER)

The main idea behind all methods is the polarization of steel by electrical current for some period, which varies depending on t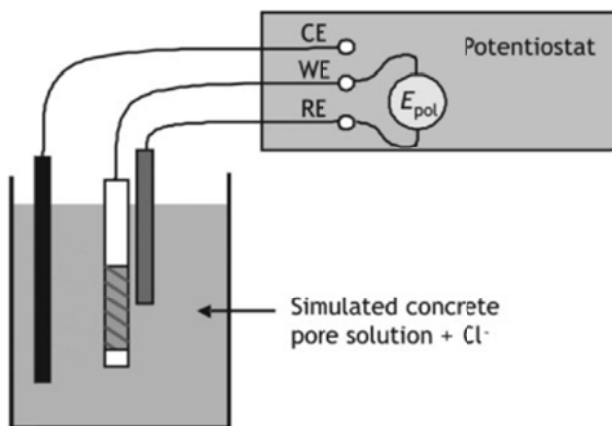he method selected and the degree of corrosion. Figure 3.5 shows the principle of an electrochemical rehabilitation method.
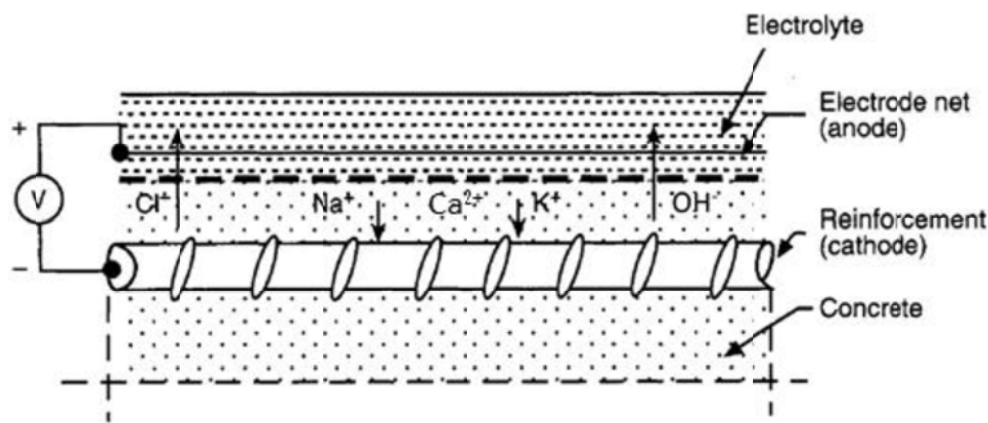
Fig. 3.5 Electrochemical rehabilitation method (from Mietz, 1998).

3.5 Corrosion initiation and chloride threshold values

The prediction of the service life of a concrete structure with embedded reinforcement steel requires the determination of the chloride threshold value C_{th}. Threshold value is the amount of chlorides needed to cause depassivation of steel or the amount of chlorides which causes noticeable corrosion from practical point of view (Angst et al., 2009).

Several parameters define the threshold values such as: concrete-steel interface, pH of the pore solution, steel potential, binder type, surface condition of the steel, moisture content, oxygen availability, water-binder ratio, resistivity, degree of hydration, type of steel, temperature, chloride source, cation accompanying the chloride ion, inhibitors and electrochemical treatment (Angst et al., 2009).

3.6 Graphene acting as a functionalized anticorrosion coating

Steel corrosion costs more than 200 billon $ every year to the US industries for repairs and replacement of corroded elements (Prasai, 2012). It is imperative to find new materials for efficient steel protection from the corrosion side effects in order to prolong their service life and have a more ecological footprint on the environment.

Graphene has attracted the scientific attention due to its extraordinary properties that place it as high priority for implementation in the concrete paste but also use it as coating on the reinforcement steel bars. Graphene's structure confers excellent carrier space to the electrons, thus shows high electron mobility at the room temperature (250.000 cm^2/V) (Geim, 2007, Singh, 2011) and ballistic transport and quantum hall effect at the room temperature. Graphene has also excellent mechanical properties, such as 1 TPa Young's Modulus and 130 GPa tensile strength (Ni et al., 2008, Mohiuddin et al., 2009). Regarding its thermal properties, the highest thermal conductivity measured at the room temperature was 5000 Wm^{-1}K^{-1} (Balandin et al., 2008).

Graphene has also barrier properties (Prasai et al., 2012, Chen et al., 2011). It has been proved that graphene is a high water and oil repellent material, while GO is hydrophilic (Chien-Te et al., 2011). This means that if graphene was used as coating it would be ideal as a water and oil resistant material. Graphene is also chemically inert and stable under 400°C, which means that it has anti-corrosion properties. For these reasons, it is suggested that graphene could become an excellent coating for steel bars, since it could work like a gas barrier impeding the oxygen and water penetration to the steel surface and prohibit any corrosion reactions.

3.7 Previous studies - Research results

➢ Single-atomic graphene films are impermeable to gas molecules (Bunch et al., 2008)

➢ Graphene can cease the oxidation of the underlying copper and nickel metals, thus work as anti-corrosion barrier (Chen et al, 2011).

➢ Prasai and his research team (Prasai et al., 2012) focused on the anti-corrosion properties of graphene and proved that single but also multi-layer graphene films can work as anti-corrosion coatings and analysed the passivation of steel coated with graphene with quantitative models. They suggest that their method could be used for all metals and for different types of surfaces; rough or smooth. The efficiency of the graphene coatings is highly dependent on the proper transfer of graphene on the metal surface, so that it covers it

homogeneously and that there is no crack on the graphene surface, where corrosion could start.

➢ Compton et al. (2010) revealed that polystyrene film (PS) with little graphene content had much lower permeability in oxygen molecules than the best results published for polymer/clay composites. Graphene would be ideal in reducing the permeability of other polymer coatings also, working as gas barrier (Chang et al., 2012).

➢ Sutter et al. (2010) investigated the efficiency of single-layer graphene on the passivation of Ru thin films. The single-layer graphene covered homogeneously and completely the Ru substrates with irregular shapes. They proved that a single-layer metal coating can protect it from gas permeability, thus metal corrosion.

4. Experiments on graphene cement nanocomposites

The experimental part consists of:

Part A: the compressive and tensile strength tests for the investigation of the compatibility between the graphene and the cement hydrates.

Part B: Open circuit potential measurement of reinforcing steel bars coated with graphene and embedded in concrete bars. The corrosion potential was measured for reference and coated with graphene bars.

Fig. 4.1 The graphene solution provided from the SHT Smart High Tech AB, Sweden

4.1 Method of production of graphene/silica hybrid sheets

The following description about the Graphene Oxide's production method was provided from SHT Smart High Tech AB:

Graphene oxide could be synthesized from graphite flakes by following the modified Hummers method. In order to obtain a well-dispersed silica coating layer, tetraalkoxysilane which may be used as the precursor of silica will be added to the alcohol while stirring on a magnetic stirrer, then followed by adding the graphene oxide aqueous dispersion, DMA solution needs to be added into the mixture to speed up the dissolution of tetraalkoxysilane. The mixture needs to be stirred at the room temperature for 30 min. The measured pH should be controlled in the range of 12.3–12.6. After surface silica coating, graphene oxide could be reduced to graphene by utilizing strong reductants in order to reform the sp2-bonded carbon crystal lattice. After reduction, graphene/silica hybrid sheets were purified by repeated washing and centrifugation with alcohol–water mixture in a volumetric ratio of 7:3.

21

4.2 Part A

4.2.1 Compressive strength tests

For Part A, the compressive strength tests do not follow any standardized method, since the specimens produced were so small and the expected compressive strength of standard specimens could not be succeeded. For this reason as well as for comparison only, different curing time periods were chosen for each test. The purpose was to compare the compressive strength between the reference mix and the mixes with graphene.

Test 1

Cement paste mixing: Three mixes were produced containing reference and different graphene contents of 0.05 and 0.1 wt% of cement. Graphene SHT G1000S was used with 1.4% solid particles, as it can be seen in the following table. Swedish Portland cement for civil engineering CEM I 42,5N BV/SR/LA was used. The mixes were prepared separately and mixed by hand and simple rotary machine.

Table 4.1 Mixture proportions for the samples

Mix No.	Cement, g	Solid particles	SHT G1000S, g	Graphene	Water, g	*w/c*
Mix 0	100	0	0	0	45	0.45
Mix 1	100	1.40%	3.58	0.05%	45	0.49
Mix 2	100	1.40%	7.15	0.10%	45	0.52

Casting and curing: The specimens were molded in small cylinder molds of 3.2 cm height and 1.6 cm diameter, as it can be seen in Figure 4.2. The specimens were left in the molds at the room temperature for 24 hrs and then cured for a period of 26 days in a water bath at room temperature. Before testing, the specimens were removed from the molds and left to dry at the room temperature. Afterwards, the specimens' plain surfaces were polished in order to have smooth and totally vertical surfaces before testing on the tensometer.
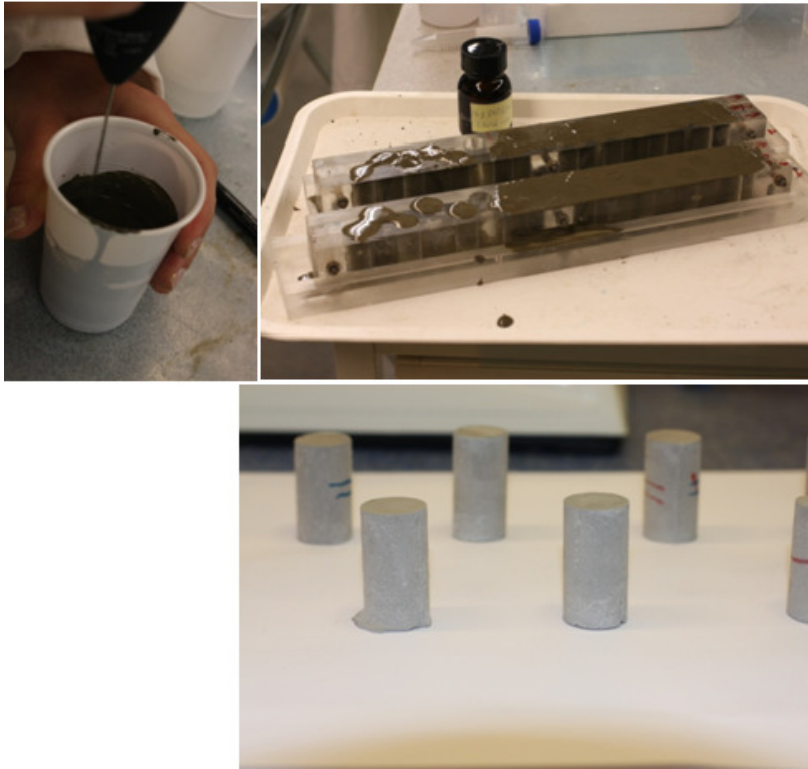
Fig. 4.2 The casting procedure and specimens before testing

Compressive strength measurements: The compressive strength test was conducted with a manual tensometer, where cyclic handle was used to apply the load. The specimens should have small size and very smooth surfaces in order to get adjusted at the grips. If defects exist at the surfaces or inclined surfaces the defects can be the cause of earlier failure and underestimation of the real compressive strength of the specimens.

Fig. 4.3 The Hounsfield manual tensometer used at the Chalmers laboratory

The following table presents the measurements in kg of the failure force applied on the specimens, the calculation of the compressive strength and the coefficient of variation for each mix.

Table 4.2 Compressive strength test measurements

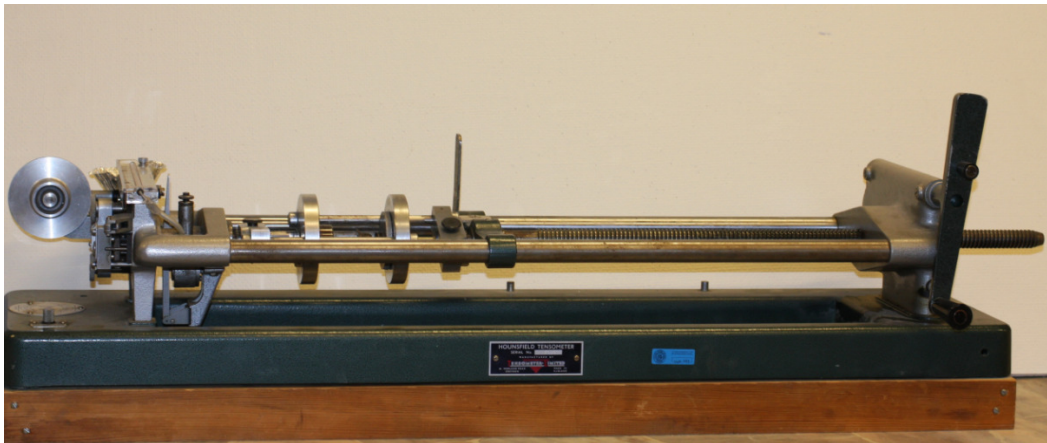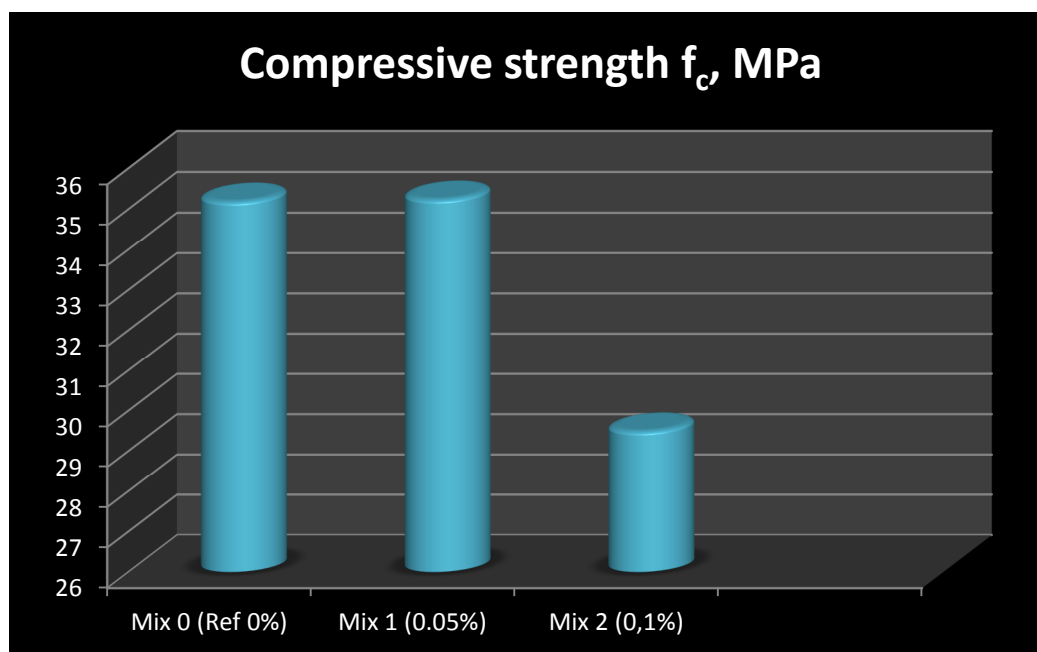| Specimen No.	Failure Force, kg		
	Mix 0 (Ref 0%)	Mix 1 (0.05%)	Mix 2 (0,1%)
1.	680	820	420
2.	890	760	550
3.	580	800	400
4.	800	640	650
5.	900	720	610
6.	810	620	560
7.	810	700	830
8.	550	850	600
9.	480	660	750
10.	720	660	680
Diameter (mm)	16	16	16
f_c, MPa	35.19	35.24	29.49
Change, %	-	0.1%	-16.2%
Coefficient of variation	20%	11%	22%

Fig. 4.4 The mean compressive strength of each mix

As it can be seen from the results above, Mix 2 demonstrated a lower compressive strength than the reference mix by 16%. This is due to the fact that the graphene solution used was saturated before mixing in the cement paste, thus it would not react with the cement hydrates. The coefficient of variation expresses the large deviation of

the results in comparison with the average strength. Therefore, the uncertainty of test results is large and no clear conclusion can be drawn.

The large deviation in all mixes can be explained by defects or not vertical surfaces of the specimens to the tensometer's grips. Also, another reason for the large deviation could be that the tensometer works manually instead of automatically. The readings of the failure force were made by operator's eyes that can introduce a big error.

Test 2

Cement paste mixing: For this experiment, we had 2 solutions: graphene-S containing silica atoms and graphene-FS with functional groups containing silica atoms. Both had solid particles 4%. Five different mixtures were produced: the reference mixture without graphene, the S1 and FS1 mixes with 0.1 wt % graphene and the S2 and FS2 mixes with 0.3 wt % graphene. The same cement as in Test 1 was used. The mixes were prepared separately and mixed by hand and simple rotary machine. At the following table are the details of the mix.

Table 4.3 Mixture proportions for the samples

Mix proportion, g						
Mix No.	Cement, g	Solid Particles	SHT G1000, g	Graphene	Water, g	*w/c*
Ref	60	4%	0	0	26.987	0.45
S1	60	4%	1.503	0.10%	25.493	0.45
S2	60	4%	4.529	0.30%	22.654	0.45
FS1	60	4%	1.5	0.10%	25.55	0.45
FS2	60	4%	4.452	0.30%	22.65	0.45

Casting and curing: The specimens were cast in the same molds as in test 1 and tested after a week. The specimens were left in the molds at the room temperature for 24 hrs and then cured for a period of 5 days in a water bath in the oven at 50°C. Before testing, the specimens were removed from the molds and left to dry at the room temperature for 24 hrs. Afterwards, the specimens were polished in order to have smooth and totally vertical surfaces before testing at the tensometer.

Compressive strength measurements: The compressive strength was defined with a manual tensometer as in Test 1. The following table presents the measurements in kg of the failure force applied at the specimens, the calculation of the compressive strength and the coefficient of variation for each mix.

Table 4.4 Compressive strength test measurements

Specimen No.	Failure Force, kg				
	Form 0 (Ref 0%)	S1	S2	FS1	FS2
1.	700	530	710	460	520
2.	520	620	620	710	770
3.	600	410	800	510	490
4.	480	250	640	550	500
Diameter (mm)	16	16.00	16.00	16.00	16.00
fc, Mpa	28.03	22.06	33.75	27.17	27.78
Change, %	-	-21.3	20.4	-3.0	-0.9
Coefficient of variation	17%	35%	12%	19%	23%
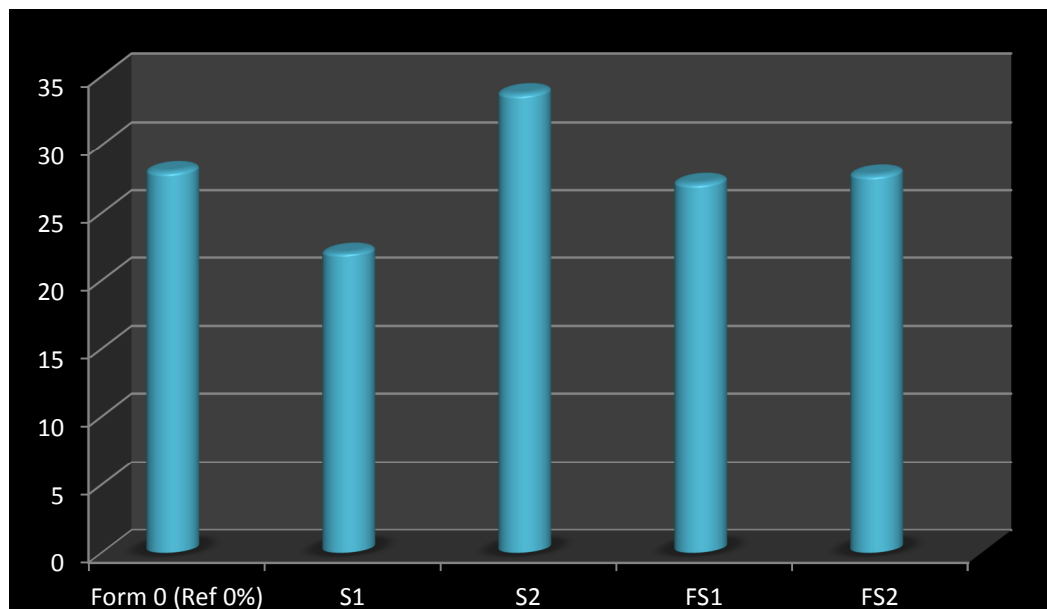
Fig. 4.5 The mean compressive strength of each mix

As it can be seen from the results above, Mix S1 demonstrated a lower compressive strength than the reference mix by 21%, whereas Mix S2 demonstrated a compressive strength by 20% higher than the reference mix.

The coefficient of variation expresses the large deviation of the results in comparison with the average strength. Similarly, the large deviation in all mixes can be explained by defects or not vertical surfaces of the specimens to the tensometer's grips. Also, operator's error in reading the failure force by eyes might be another reason. Again, the uncertainty of test results is large and no clear conclusion can be drawn.

Casting and curing:

The standard compressive strength test of EN 196-1 was followed. At this experiment two mixes were produced: the reference mortar without graphene called Mortar-R and the mortar with 0.68% graphene from a solution with 5% solid particles and water/cement=0.5 called Mortar-G. The same cement as in Tests 1 and 2 was used. CEN Standard sand of 0-4 mm was used with cement:sand=1:3. Due to limited quantity of graphene, instead of three only two specimens with graphene were cast with sand of 1350*2/3=900g. The reference specimens were cast according to the EN 196-1. The mixture was mixed mechanically and two specimens with graphene and three reference specimens without graphene were cast. At the following table are the details of the mix:

Table 4.5 Mixture proportions for the samples

Mix No.	Cement(g)	Solid (%)	SHT G1000S (g)	Graphene (%)	Water (g)	w/c
Mortar-R	450	0	0	0.00%	225	0.50
Mortar-G	300	5.0%	41	0.68%	111	0.50

Prior to the mixing, graphene and water were firstly mixed and treated by ultrasonication on a Brandson Sonifier for better dispersion. The specimens were cast in standard prismatic forms of sizes 40×40×1600 mm after mixing and cured for 28 days before testing. The specimens were left in the forms covered with plastic sheet for 24 h and then the demoulded specimens were immersed in water until strength testing at the age of 28 days. The prismatic test specimens can be seen in Figure 4.6.

Fig. 4.6 The specimens before testing

One day before testing the specimens were removed from water. The specimens were first bending-tested to find their flexural strength and broken in two halves. After the bending test, only the one half of each specimen was tested to find their compressive strength.

4.3.1 Bending test for flexural strength

Fig. 4.7 The bending test machine for flexural strength

Figure 4.7 shows the specimen before the test initiation (left) and after the bending failure (right). The bending stress causing failure was marked on the white ruler at the end of the experiment. The test procedure is in accordance with EN 196-1.

Table 4.6 Results from the flexural strength test

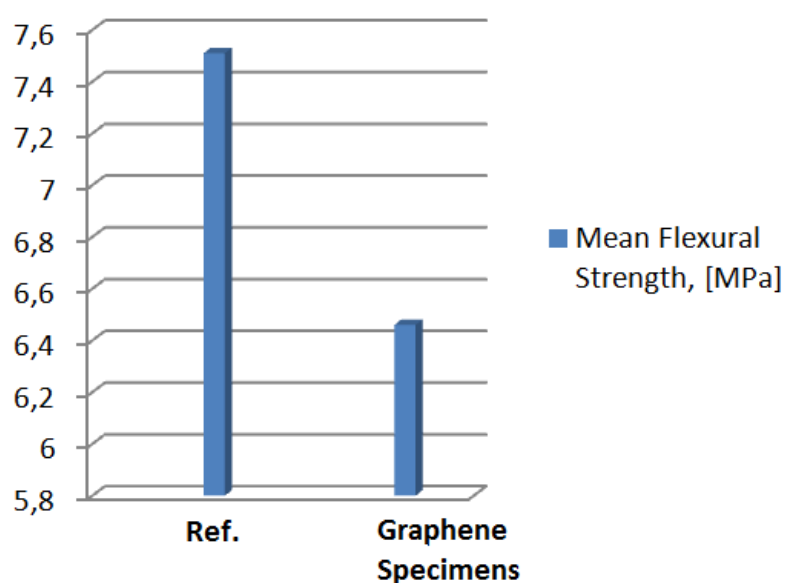| Reference specimens	max flexural stress [kp/cm^2]	flexural strength [MPa]
R1	84.2	8.26
R2	69.3	6.79
R3	76.2	7.48
Average	76.56	7.51
Stad. dev.		0.73
COV		9.7%
Graphene specimens	max flexural stress [kp/cm^2]	flexural strength [MPa]
G1	64	6.28
G2	67.8	6.65
Average	65.9	6.46
Std. dev.		0.26
COV		4.1%

Fig.4.8 The mean flexural strength test results

The average flexural strength value for the reference specimens is 7.51 MPa and the respective value for the graphene specimens is 6.46 MPa. Thus, the average flexural strength of the graphene specimens is about 14% lower than the reference ones.

4.3.2 Compressive strength test

The following standardized compressive strength machine was used to identify the compressive strength of the specimens. All parameters were input to the program of the machine at the beginning and the compressive force was recorded. The test procedure is in accordance with EN 196-1.

Table 4.7 Results from the compressive strength test

Specimens	F_m (kN)	$\sigma_m[\frac{N}{mm^2}]$
R2	108.4	67.75
R3	95.33	59.58
Average	101.4	63.38
Std. dev.		4.11
COV		6.4%
G1	106.98	66.86
G2	106.5	66.56
Average	106.74	66.71
Std. dev.		0.21
COV		0.22%

Figure 4.9 The compression machine for compressive strength test

Finally, the mean compressive strength of the graphene specimens was increased by 5.25% compared with the mean strength of the reference specimens.

It is believed that this type of graphene may have no interaction with cement hydrates but acted as a separation material resulting in a decrease in flexural strength, whereas acted as a hard filler resulting in a slight increase in compressive strength.

4.4 Part B - Corrosion test

The corrosion test was performed in order to investigate the effect of graphene used as anti-corrosion coating on the reinforcement steel bars, embedded in cement mortar.

Experiment description

The ribbed steel bars with diameter 10 mm under "as received" condition with arbitrary degree of superficial corrosion were used in order to approach more the industrial conditions and make a feasibility study on the graphene's efficiency. Ten steel bars were prepared by making a hole on the top of the steel bar in order to connect them with working cables afterwards. After that, one end of each steel bar was coated with cement paste of water/cement = 0.45, to about 2 cm high from the bottom, see Figure 4.10. Then the steel bars were hung in wet environment for 3 days. The next step was the application of graphene, simply by brushing a very thin layer of the graphene solution on five of the randomly chosen steel bars.
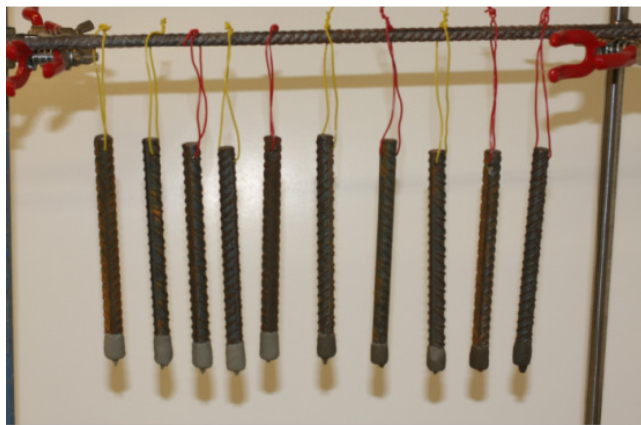
Fig. 4.10 Preparation of the steel bars

After hanging to dry for an hour, 10 mortar specimens with steel bar in each were cast in such a way as shown in Figure 4.11, where the steel bars were centrally and vertically positioned in the specimens with the help of the vertically positioned moulds (plastic tubes).

Cement Mortar Details: Swedish Portland cement for civil engineering CEM I 42.5N BV/SR/LA was used. The proportions were: water:cement:sand = 0.45:1:2.

Table 4.8 The mix proportions of mortar

Mix proportions		
Water, g	Cement, g	Sand(<1mm), g
315	700	1400

The specimens had cylinder shape of 3 cm diameter and 15 cm length. Specimens 1-5 had no graphene coating, whereas specimens 6-10 had graphene coating.
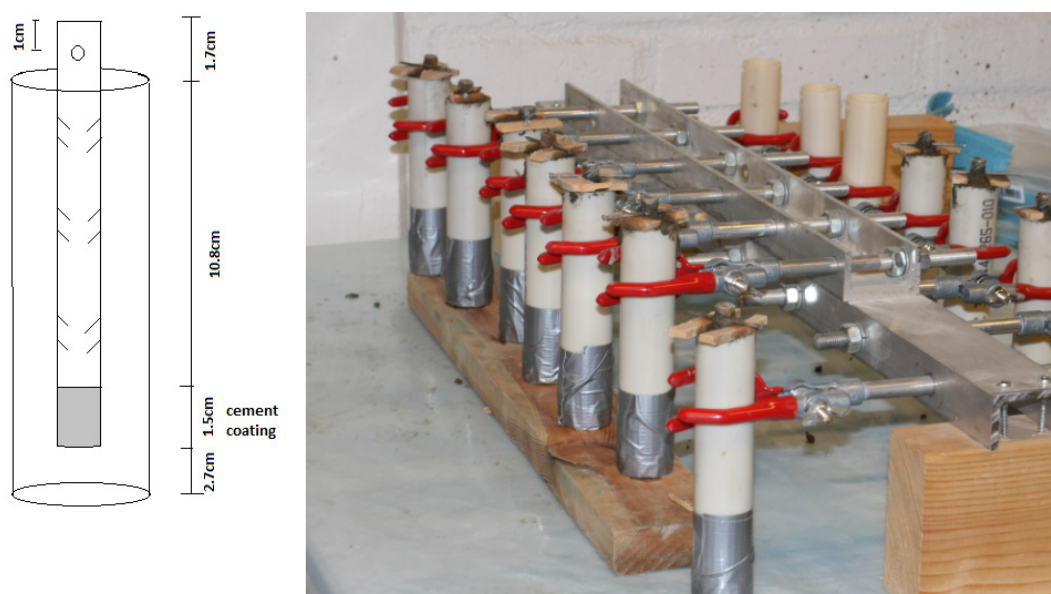
Fig. 4.11 Sketch of the specimens and curing

After 24 hrs the specimens were put in a moist environment for 14 days. Then, the specimens were taken out of the moist environment. The plastic tubes were removed and the physical state of the specimens was evaluated summarized in Table 4.9 and shown in Figure 4.12. As can be seen, there are some cracks (due to hydration shrinkage) and air voids (due to poor compaction without vibration) on the surfaces of specimens.

Table 4.9 Specimens' physical state

Specimen No.	Cracks	Surface holes
1.	Small	small
2.	1 medium diagonal	medium
3.	1 medium vertical+1big & more small diagonal	medium
4.	1 medium diagonal	small
5.	1 medium diagonal	small to medium
6.	No	huge
7.	1 big all around + 1 small diagonal	big
8.	1 all around	big
9.	No	huge
10.	3 medium	medium
Specimens		
1.-5.	Without graphene	
6.-10.	Coated with graphene	
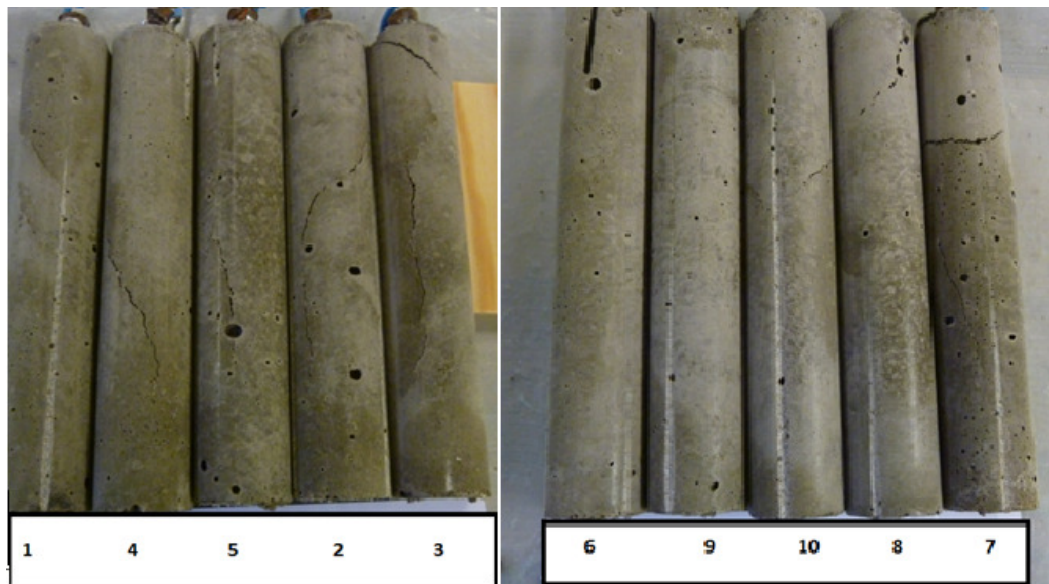
Fig. 4.12 Specimens' condition (obvious cracks and holes)

Finally, only the bars 1, 2, 4, 5 as reference and 6, 8, 9, 10 as graphene coated were used for the experiment because they were in relatively better conditions. These specimens were immersed in an epoxy solution with NM Injektering INP42 and hardener with the weight ratio 2:1 for 3 days. After the hardening of epoxy resin the specimens were cut to expose only one flat surface of each specimen whilst the other surfaces were protected with epoxy. Due to some bubbles created in epoxy which was captured by the air voids, a new epoxy solution with the same proportions was

brushed carefully to cover these defects also at big pores of the exposed surface, see Figure 4.13. The specimens were put in a moist environment while the epoxy became hardened.
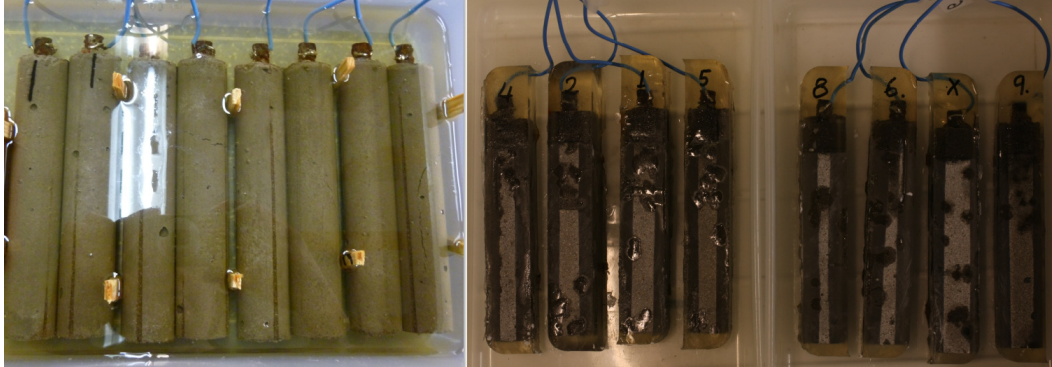

Fig. 4.13 Specimens immersed in an epoxy solution (left), cut specimens with an exposed flat surface and treated with epoxy at defected points (right)

After 3 days, the specimens were put vertically in a chloride solution with 6 wt% NaCl. A data-logger was used to register corrosion potentials of each specimen by connecting the working cable to each channel and a reference electrode to the common ground. The data were recorded every 15 min for 25 days until every bars were under the depassivation. The reference electrode used in the experiment was a type of manganese dioxide with commercial name ERE 20, manufactured by FORCE Technology in Denmark. This reference electrode was calibrated by a saturated calomel electrode and then the potential values were converted to those against the copper-copper sulfate electrode (CSE).
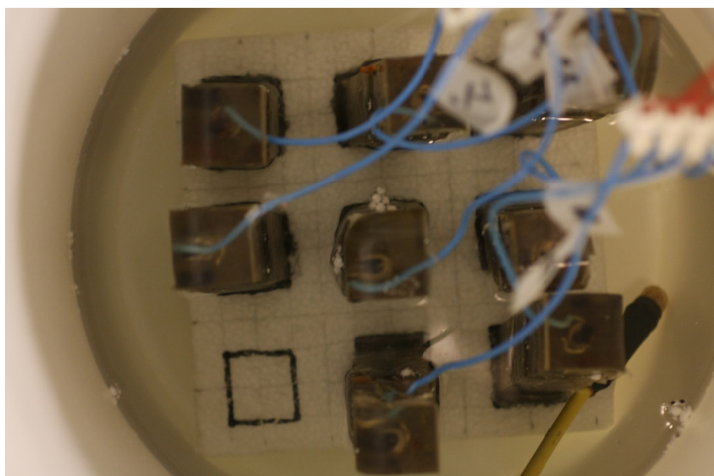

Fig. 4.14 Half-cell potential experiment

Fig. 4.15 shows the potential curves of each specimen in time. Abrupt decrease in potential of the order of 150 mV indicates that corrosion has taken place. According to the American standards ASTM C 876 for the corrosion initiation, potential values under 350 mV CSE, means that there is higher than 90% possibility of corrosion.
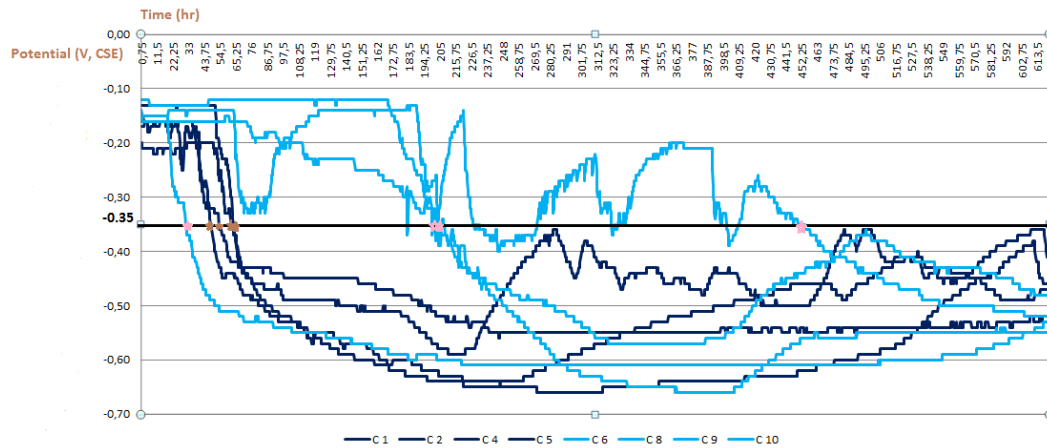
Fig. 4.15 The potential curves of the specimens

Results Analysis

As it can be seen in Figure 4.15 and the following summarizing table 4.10, the specimens with graphene coating revealed a delayed corrosion initiation.
Especially specimen 8 lasted longer than all the other specimens and displayed some repassivation-depassivation cycles, as a result of the higher amount of chlorides needed for the depassivation of the passive film.

The bar in specimen 9 with graphene coating corroded first, possibly due to surface defects and cracks, which were not fully repaired with epoxy.

Table 4.10 Corrosion initiation time

Specimen No.	Time (hrs)
C1	53.75
C2	61.75
C4	48
C5	63.5
C6	202.25
C8	449.75
C9	31.25
C10	199.75

Finally, the corroded steel bars were released from the specimens at the end of the experiment for visual observation. Figure 4.16 shows the corroded areas. As it can be seen from Fig. 4.16, the corrosion spots can be found in all the specimens, frequently at the interface between the cement paste at the end of the steel bar due to potential difference in this area.
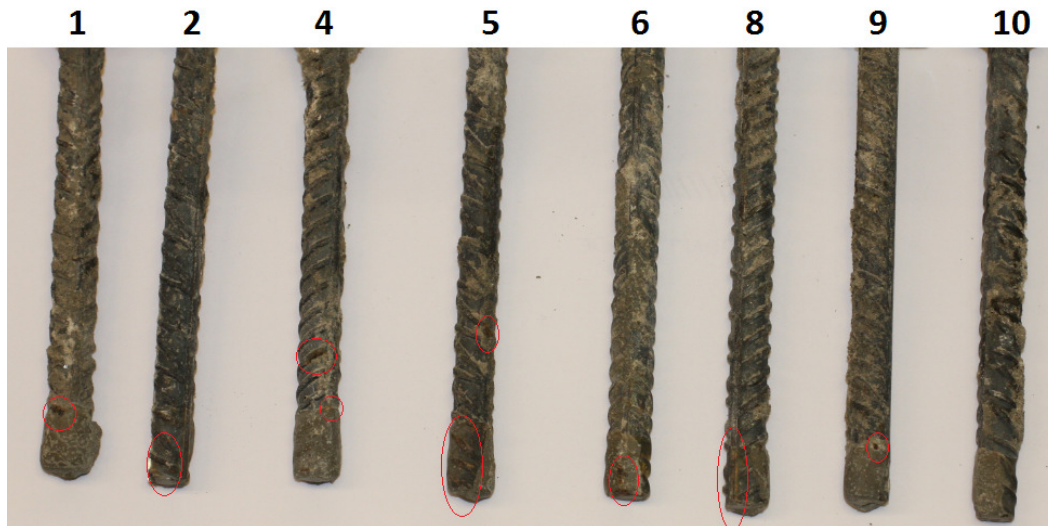

Fig. 4.16 Corroded areas of steel bars after the corrosion test

5. Conclusions and Suggestions

5.1 Concluding remarks

The exceptional properties of graphene have attracted the scientific interest for the integration of its properties to the nanocomposite materials. So far the research has focused on Carbon Nanotubes (CNTs) and Carbon Nanofibers (CNFs). The objective of this dissertation work was to study the feasibility of graphene with cement hydrates to improve the mechanical properties of cement and with reinforcement steel used as coating against corrosion.

In this direction, thorough study of the existing literature was substantial for understanding the structure of the cement hydrates and finally the structure of graphene and other graphene derivatives. One of the main tasks was to study how graphene and the cement hydrates can interact in order to obtain cement with higher mechanical properties, such as increased tensile strength.

Regarding the effect of graphene in cement, according to other studies 1.5wt% GO with 0.5wt% superplasticizer had revealed 48% higher tensile strength compared with cement mixture without GO. For the same study, the FE-SEM images showed good bonding between GO and the cement particles and the XRD diffraction data revealed increased amount of C-S-H gel in the GO modified cement nanocomposite compared with the pure cement mortar. Another study showed that the MWCNTs cement nanocomposites present early age strength and long term durability. Finally, a team of scientists investigated several functional groups of graphene and calculated the interfacial strength between the G(OH) and the C-S-H gel [(C-S-H)-G(OH)-C-S-H] 13.5 GPa compared to pristine graphene [(C-S-H)-G()-C-S-H], which was 1.2 GPa. It seems that the proper functionalization can significantly increase the compatibility of C-S-H gel with graphene, thus refine the C-S-H gel's structure from the nano-level.

Apart from the literature study some experiments were carried out for examining the mechanical strength of specimens containing graphene. These included compressive and flexural strength tests. The experimental results did not reflect the results recorded in the literature study, mainly because the graphene solution provided contained functional groups with silicon oxides, which according to ^{29}Si NMR analysis were polymerized and inactive for chemical interaction with the cement hydrates.

The procedure of graphene production is both time-consuming and expensive, which restricted the range and number of the experiments for this thesis work. However, new production techniques promise bulk production at low costs for industrial use of graphene in the future.

Graphene has also excellent electrical properties, which make it ideal candidate for use as anti-corrosion coating on the surface of steel reinforcement bars. The literature

study showed that single but also multi-layer graphene can work as anti-corrosion coatings with the possibility to have the same efficiency in different types of surfaces; rough or smooth. It has been reported that monolayer graphene films are impermeable to gas molecules and that graphene can cease the oxidation of the underlying copper and nickel metals, thus work as anti-corrosion barrier. The half-cell potential experiment conducted in this thesis work indicated that the specimens with graphene coating revealed a delayed corrosion initiation and some repassivation-depassivation cycles, as a result of the higher amount of chlorides needed for the depassivation of the passive film.

The successful implementation of graphene in cementitious materials and steel coatings could enhance their mechanical properties significantly and also prolong their service life. The ASCE Report Card for America's infrastructure in 2009 claimed that 2.2 trillion U.S.$ needed to be invested in the next 5 years in order 'to bring the nation's infrastructure to a good condition'. Thus, functionalized graphene implemented in construction materials could be the key for economic growth and sustainable development in the future.

5.2 Further research needs

There are a lot of knowledge gaps, which need to be addressed and further investigated in order to understand the mechanisms between the graphene and C-S-H gel interaction. The graphene nanomaterials could be further enhanced and used in a lot of applications if their structures and behavior are fully understood.

First of all, graphene should be efficiently dispersed within the cement matrix, making its surfaces more hydrophilic and functionalized with the desirable functional groups which will react with the cement hydrates to reinforce their bonds at the nano-scale. The proper concentration of functional groups on the graphene's surface would provide improved interfacial stiffness, strength, thermal and electrical conductivity etc. to the graphene-cement nanocomposites (Sadiq, 2013).

Additionally, graphene models should be developed with the C-S-H gel in order to calculate the interfacial strength and further study the graphene's effects from nano- to micro-scale. The chemical reactions between the graphene nanoparticles and the C-S-H gel or the reactions taking place during corrosion need to be further investigated.

There is limited research study so far on graphene's applications in cementitious materials and reinforcement steel, but the future is promising. The research community has focused on the graphene's extraordinary properties and it is expected to have great progress towards this direction in the future. Graphene should not only be limited to the mechanical or anti-corrosive and self-healing properties, but also be expanded to its environmental benefit, since it is a stable material without dangerous chemicals, as a lot of other steel coatings include and it could prolong the civil

structures' service life significantly, thus reduce the cement's production needed and the air pollution of the construction industries. Another important aspect which needs to be further investigated in graphene applications is its Life Cycle Assessment (LCA). Through life cycle assessment, the environmental impact in terms of carbon dioxide emissions and cost effectiveness are evaluated from the production phase to the end of use. The little quantity of graphene could improve or even replace the traditional reinforcement and also improve the mechanical properties of cement and electrical properties of steel with less cost and less carbon dioxide emissions in total.

6. References

Alvarez M.G. and Galvele J.R. (1984) The mechanism of pitting of high purity iron in NaCl solutions. Corrosion Science, Vol. 24, No. 1, pp. 27-48.

Angst U., Elsener B., Larsen C.K. and Vennesland Ø. (2009) Critical chloride content in reinforced concrete - A review. Cement and Concrete Research, Vol. 39, No. 12, pp. 1122-1138.

Arup H. (1983) The mechanisms of protection of steel by concrete, in Corrosion of Reinforcement in Concrete Construction. A.P. Crane, Society of chemical industry, Ellis Horwood Limited, pp. 151-157.

Alkhateb, H., Al-Ostaz, A., Cheng, A., and Li, X. (2013). Materials Genome for Graphene-Cement Nanocomposites. *J. Nanomech. Micromech.*, Vol. 3, No. 3, pp. 67–77.

Babak F., Hassani Abolfazl, Rashidi Alimorad, and Ghodousi Parviz (2014) Preparation and Mechanical Properties of Graphene Oxide: Cement Nanocomposites. The Scientific World Journal, Vol. 2014, Article ID 276323, 10 pages.

Balandin AA, Ghosh S, Bao W, Calizo I, Teweldebrhan D (2008) Superior thermal conductivity of single-layer graphene. Nano Lett 8, pp. 902-907.

Bertolini L, Elsener B, Pedeferri P and Polder R (2004) Corrosion of steel in concrete -prevention, diagnosis and repair, 1st edition, Wiley-VCH, Weinheim, Germany.

Boukhvalov, D. W. and Katsnelson, M. I. J. Am. (2008) Chem. Soc. , Vol. 130, pp. 10697–10701

Bunch, J. S.; Verbridge, S. S.; Alden, J. S.; van der Zande, A. M.; Parpia, J. M.; Craighead, H. G.; McEuen, P. L. (2008) Impermeable Atomic Membranes from Graphene Sheets. Nano Lett., Vol. 8, pp. 2458–2462.

Chang C., Huang T., Peng C., Yeh T., Lu H., Hung W., Weng C., Yang T., Yeh J. (2012) Novel anticorrosion coatings prepared from polyaniline / graphene composites. Elsevier, Carbon, Vol. 50, pp. 5044-5051.

Chen, J. J., Thomas, J. J., Taylor, H. F. W., and Jennings, H. M. (2004) Solubility and structure of calcium silicate hydrate." Cement Concr. Res.0008-8846, Vol. 34, No. 9, pp. 1499–1519.

Chen S., Brown L., Levendorf M., Cai W., Ju SY, Edgeworth J. et al. (2011) Oxidation resistance of graphene-coated Cu and Cu/Ni alloy. ACS Nano, Vol. 5, pp. 1321-1327.

Cheng YF and Luo JL (1999) Metastable pitting of carbon steel under potentiostatic control. Journal of The Electrochemical Society,Vol. 146, No. 3, pp. 970-976.

Chien-Te Hsieh, Wei-Yu Chen (2011) Water/oil repellency and work of adhesion of liquid droplets on graphene oxide and graphene surfaces. Surf Coatings Technol, Vol. 205, pp. 4554–61.

Compton O.C., S. Kim, C. Pierre, J.M. Torkelson, S.T. Nguyen (2010) Crumpled graphene nanosheets as highly effective barrier property enhancers. Adv Mater., Vol. 22, pp. 4759–4763.

Domone P. and Illston J. (2010) Construction materials, 4th edition, Spon Press.

EN 196-1 (2008) Methods of testing cement - Part 1: Determination of strength.

Gao, X., Jang, J., and Nagase, S. J. (2010) Phys. Chem. C , Vol. 114, pp. 832–842

Geim A. K. and Novoselov K. S. (2007) The rise of graphene. Nature Materials 6, pp. 183 – 191.

Hsiao Min-Chien, Shu-Hang Liao, Ming-Yu Yen, Po-I Liu, Nen-Wen Pu, Chung-An Wang, and Chen-Chi M. Ma (2010) Preparation of Covalently Functionalized Graphene Using Residual Oxygen-Containing Functional Groups. ACS Applied Materials & Interfaces, Vol. 2, No. 11, pp. 3092-3099.

Jennings, H. M. (2000) A model for the microstructure of calcium silicate hydrate in cement paste. Cement Concr. Res.0008-8846, Vol. 30, pp. 1.

Kim H.W., Y. Miura, C.W. Macosko (2010) Graphene/polyurethane composites for improved gas barrier and electrical conductivity.Chem Mater,Vol. 22, pp. 3441–3450.

Konsta-Gdoutos M. S., Metaxa Z. S. and Shah S. P. (2010) Multi-scale mechanical and fracture characteristics and early-age strain capacity of high performance carbon nanotube/cement nanocomposites. Cement and Concrete Composites, Vol. 32, No. 2, pp. 110–115.

Lerf A., He H., Forster M. and Klinowski J.(1998) Structure of Graphite Oxide Revisited. J. Phys. Chem. B, Vol. 102, pp. 4477-4482.

Manzano H., Ayuela A. and Dolado J. S. (2007) On the formation of cementitious C-S-H nanoparticles. The Journal of Computer-Aided Materials Design, Vol. 14, No. 1, pp. 45-51.

Mietz J. (1998) Electrochemical rehabilitation methods for reinforced concrete structures, European Federation of Corrosion Publications 24, London, UK.

Mohiuddin TMG, Lombardo A, Nair RR, Bonetti A, Savini G, Jalil R, et al. (2009) Uniaxial strain in graphene by Raman spectroscopy: G peak splitting, Gróneisen parameters, and sample orientation. Phys Rev B Condens Matter Mater Phys, 79:205433.

Ni ZH, Yu T, Lu YH, Wang YY, Feng YP (2008) Uniaxial strain on graphene: Raman spectroscopy study and band-gap opening. ACS Nano 2, pp. 2301-2305.

Peigney A., Laurent C., Flahaut E., Bacsa R.R., Rousset A. (2001) Specific surface area of carbon nanotubes and bundles of carbon nanotubes. Carbon, Vol. 39, pp. 507–514.

Petrunin S., Vaganov V., Sobolev K. (2013) The effect of functionalized carbon nanotubes on the performance of cement composites. Nanocon, Brno, Czech Republic, EU.

Pickering HW and Frankenthal RP (1972) On the mechanism of localised corrosion of iron and stainless steel, Journal of The Electrochemical Society, Vol. 119, No. 10, pp. 1297-1304.

Prasai D., Tuberquia J. C., Harl R. R., Jennings G. K., and Bolotin K. I. (2012) Graphene: Corrosion-Inhibiting Coating. ACS Nano, Vol. 6, No. 2, pp. 1102-1108.

Richardson, I. G. (1999) The nature of C-S-H in hardened cements. Cement Concr. Res.0008-8846, Vol. 29, No. 8, pp. 1131–1147.

Sadiq M. (2013) Reinforcement of cement-based matrices with graphite nanomaterials. Ph.D Thesis. Michigan State University, Michigan, USA.

Sedaghat A., Ram M., Zayed A., Kamal R. and Shanahan N. (2014) Investigation of Physical Properties of Graphene-Cement Composite for Structural Applications. Open Journal of Composite Materials, Vol. 4, No. 1, pp. 12-21.

Sobolev K. and Gutierrez M. F. (2005) How nanotechnology can change the concrete world. American Ceramic Society Bulletin, Vol. 84, No. 10.

Silva N. (2013) Chloride induced corrosion of reinforcement steel in concrete-Threshold values and ion distributions at the concrete-steel interface. PhD Thesis. Chalmers University of Technology, Gothenburg, Sweden.

Singh V., Joung D., Zhai L., Das S., Khondaker S.I., Seal S. (2011) Graphene based materials: Past, present and future. Prog Mater Sci., Vol. 56, pp. 1178–271.

Sobolev K., Shah S.P. (2008) SP-254 Nanotechnology of concrete: recent developments and future perspectives. American Concrete Institute, Detroit.

Strehblow H-H (2002) Mechanisms of Pitting Corrosion, in Corrosion Mechanisms in Theory and Practice, 2nd edition (P. Marcus), Marcel Dekker Inc., New York, USA.

Sutter E., Albrecht P., Camino F. E., Sutter P. (2010): Monolayer graphene as ultimate chemical passivation layer for arbitrarily shaped metal surfaces. Elsevier. Carbon, Vol. 48, No. 15, pp. 4414–4420.

Tong Y., Bohm S. and Song M. (2014) Graphene based materials and their composites as coatings. Austin J Nanomed Nanotechnol., Vol.1, No. 1, pp. 16.

Van Damme H. and Gmira A. (2006) cement hydrates. Handbook of clay science. Elsevier, Boulevard, UK, pp. 1113-11127.

Vennesland Ø., Raupach M. and Andrade C. (2007) Recommendation of RILEM TC 154-EMC: Electrochemical techniques for measuring corrosion in concrete - measurements with embedded probes, Materials and Structures, Vol.40, No.8, pp. 745-758.

Warner J. H., Schaffel F., Rummeli M., Bachmatiuk A. (2013) Graphene: Fundamentals and emergent applications.

Wei, W. and Qu, X. (2012), Extraordinary Physical Properties of Functionalized Graphene. Small, Vol. 8, pp. 2138–2151.

Zhu Y., Murali S., Cai W., Li X.G., Suk J. W., Potts J. R. and Ruoff R. S. (2010) Graphene and graphene oxide:synthesis, properties and applications. Adv.Mater., Vol. 22, pp. 3906-3924.

Appendix A: Half-cell potential measurements

The half-cell potential measurements are given below:

Time (hr)	C1	C2	C4	C5	C6	C8	C9	C10
0	-0.13	-0.16	-0.14	-0.11	-0.1	-0.15	-0.12	-0.15
24	-0.16	-0.21	-0.16	-0.13	-0.13	-0.14	-0.29	-0.16
48	-0.32	-0.2	-0.35	-0.13	-0.12	-0.14	-0.49	-0.16
72	-0.43	-0.44	-0.48	-0.44	-0.12	-0.32	-0.53	-0.16
96	-0.44	-0.47	-0.53	-0.52	-0.12	-0.2	-0.54	-0.2
120	-0.45	-0.49	-0.55	-0.56	-0.13	-0.15	-0.55	-0.23
144	-0.45	-0.5	-0.57	-0.59	-0.12	-0.14	-0.56	-0.23
168	-0.47	-0.51	-0.6	-0.61	-0.12	-0.14	-0.58	-0.27
192	-0.5	-0.55	-0.61	-0.63	-0.26	-0.24	-0.59	-0.33
216	-0.53	-0.59	-0.63	-0.64	-0.41	-0.17	-0.6	-0.39
240	-0.55	-0.51	-0.64	-0.65	-0.46	-0.38	-0.61	-0.48
264	-0.55	-0.41	-0.65	-0.63	-0.49	-0.37	-0.61	-0.54
288	-0.55	-0.39	-0.66	-0.6	-0.51	-0.27	-0.61	-0.61
312	-0.55	-0.42	-0.66	-0.57	-0.56	-0.25	-0.61	-0.63
336	-0.55	-0.44	-0.65	-0.55	-0.57	-0.31	-0.61	-0.65
360	-0.55	-0.46	-0.64	-0.53	-0.57	-0.22	-0.61	-0.65
384	-0.55	-0.48	-0.64	-0.51	-0.57	-0.21	-0.61	-0.66
408	-0.54	-0.44	-0.64	-0.49	-0.54	-0.36	-0.61	-0.65
432	-0.54	-0.5	-0.63	-0.48	-0.47	-0.3	-0.61	-0.6
456	-0.55	-0.5	-0.62	-0.46	-0.43	-0.36	-0.61	-0.56
480	-0.54	-0.37	-0.6	-0.48	-0.4	-0.41	-0.61	-0.56
504	-0.54	-0.38	-0.59	-0.44	-0.38	-0.44	-0.61	-0.55
528	-0.54	-0.42	-0.55	-0.41	-0.41	-0.47	-0.6	-0.55
552	-0.54	-0.43	-0.49	-0.45	-0.44	-0.5	-0.59	-0.55
576	-0.54	-0.46	-0.45	-0.42	-0.44	-0.5	-0.58	-0.55
600	-0.53	-0.49	-0.4	-0.37	-0.46	-0.51	-0.56	-0.55
620.25	-0.53	-0.47	-0.46	-0.41	-0.48	-0.52	-0.53	-0.55

Appendix B:

NMR GS im - tool was used for ^{29}Si NMR spectroscopy experiment for the graphene solution provided for Test 2. The graph below shows that the S-solution contains silica. but the FS-solution does not contain silica at all.

Testing Materials:

- Sample 1: S-solution
- Sample 2: FS-solution
- Silica powder and silica were used as reference materials.